

The Pennsylvania State University

The Graduate School

College of Engineering

**DEVELOPMENT OF AN IMPROVED ALGORITHM FOR
WORKPIECE LOCALIZATION OF RAW MATERIAL**

A Thesis in

Industrial Engineering

by

Yu Ma

© 2015 Yu Ma

Submitted in Partial Fulfillment
of the Requirements
for the Degree of

Master of Science

August 2015

The thesis of Yu Ma was reviewed and approved* by the following:

Sanjay Joshi

Professor of Industrial Engineering

Thesis Adviser

Robert C. Voigt

Professor of Industrial Engineering

Harriet Black Nembhard

Professor of Industrial Engineering

Head of the Department of Industrial Engineering

*Signatures are on file in the Graduate School.

ABSTRACT

One of the problems that manufacturing industries are faced with is the proper localization of workpieces within the raw blanks while maintaining sufficient machining allowances. This is especially important in case where the raw material is of near net shape. The solution of this problem is defined as workpiece localization. The corresponding decision-making is especially critical when the size and shape of the blank are closely specified to the designed model to ensure sufficient material.

In this paper, we present an improved workpiece localization algorithm for machining, which is achieved by two-step point cloud localization. Firstly, the two point clouds are created (one for the part and one for workpiece) and localized roughly by the Principal component analysis algorithm. Secondly, a more precise algorithm, i.e., least square-based algorithm, is used to search for the best translation and rotation of the workpiece within the blank. The algorithm allows an optimal setup of the part to ensure that no shortage of material occurs during machining. Through transformation, the algorithm determines whether or not the designed model is totally enclosed in the actual raw material to be machined. The two-step localization algorithm can reduce the computational time. The input to the new algorithm is simplified for a 2D workpiece localization process by using point clouds. A 2D example of plasma cutting of the blank and subsequent machining is used to test the algorithm. The results show the processing time is faster than other localization methods using the simplified inputs.

TABLE OF CONTENTS

List of Figures	v
List of Tables.....	vi
Acknowledgements.....	vii
Chapter 1 Introduction	1
1.1 Background.....	1
1.2 Automatic Workpiece Localization	4
1.3 Problem Statement.....	5
Chapter 2 Literature Review	7
2.1 Iterative Closest Point Algorithm	7
2.2 Geometric Algorithms for Workpiece Localization	10
2.3 Feature Based Workpiece Localization Algorithm	12
Chapter 3 Development of the Improved Algorithm for Workpiece Localization.....	14
3.1 Algorithm Introduction.....	14
3.2 Preprocessing of Point Cloud Data.....	16
3.3 Rough Localization of Measured Point Cloud	16
3.4 Precise Localization of Measured Point Cloud	20
Chapter 4 Result and Conclusion.....	27
4.1 Example of Workpiece Localization Algorithm.....	27
4.2 Comparison of the new algorithm and previous algorithm	30
4.3 Conclusion	33
References	34
Appendix A Dataset of Original Point Clouds	39
Appendix B Code of the Algorithm.....	45

LIST OF FIGURES

Figure 1.1 Workpiece localization process	2
Figure 3.1 Flowchart of machining allowance evaluation.....	15
Figure 3.2 Original scanned data (a); After-processed data (b); discretized reference model (c)	17
Figure 3.3 Flow chart of the workpiece localization algorithm.....	25
Figure 4.1 Original location (a); center-superposed point clouds (b); rough localization result (c).....	28
Figure 4.2 Precise localization result	29
Figure 4.3 Result with insufficient machining allowance	30
Figure 4.4 Convergence of different methods	32

LIST OF TABLES

Table 4.1 Comparisons between different algorithms	31
--	----

ACKNOWLEDGEMENTS

It would not have been possible to finish my thesis without a great deal of guidance and support from the people around me. I would like to deeply thank those people who, during the several months in which this project lasted, provided me with everything I needed.

First of all, I would like to express my deepest appreciation to my committee chair, Professor Sanjay Joshi for his guidance, advice and support during the entire project. I have benefited greatly from his outstanding insight and rigorous research attitude. Without his guidance and persistent help, this thesis would not have been possible.

I would also like to give special thank to the members of my thesis committee for their support: Professor Robert C. Voigt and Professor Harriet Black Nembhard.

Finally, I owe huge gratitude to my parents for their financial and mental support of my graduate study. Without their selfless and endless help, I would not have the chance to study in the Pennsylvania State University.

Chapter 1

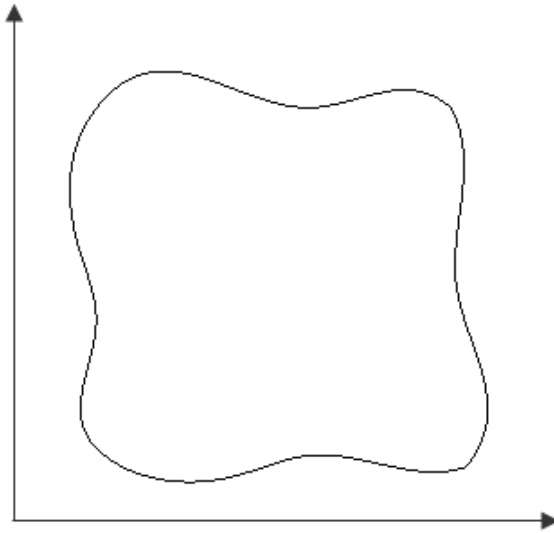
Introduction

1.1 Background

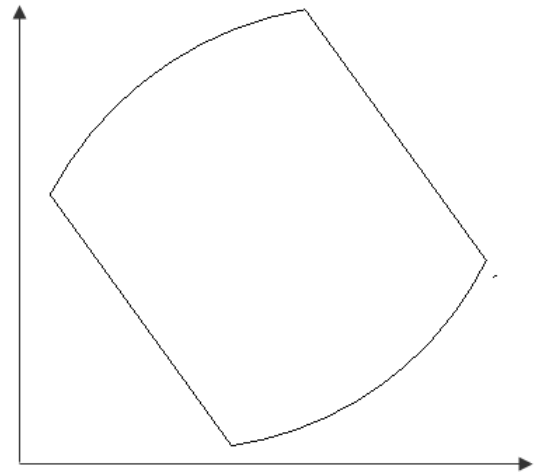
In the manufacturing industry, one critical problem of machining is the proper localization of the designed part relative to the raw material. To obtain the expected part successfully, the designed part must be enclosed in the raw material with sufficient machining allowance. The machining allowance is a planned deviation between an actual dimension and a theoretical dimension, or between an intermediate-stage dimension and an intended final dimension. The machining allowance is contrasted with a tolerance, which accounts for expected but unplanned deviations. The inspection for the machining allowance of raw material, which is also defined as workpiece localization, is significantly important, since it ensures there is enough material available for machining

Workpiece localization is defined as the following: given a rigid raw material arbitrarily placed in a coordinate system, the position and orientation of the corresponding final machined part within the raw material needs to be determined relative to the raw material, with sufficient machining allowance. This ensures that there is no material shortage in the raw material. Consider a raw material that is randomly placed on the coordinate system as shown in Fig 1.1(a). We wish to transform the reference model's position and orientation relative to the raw material to ensure that no

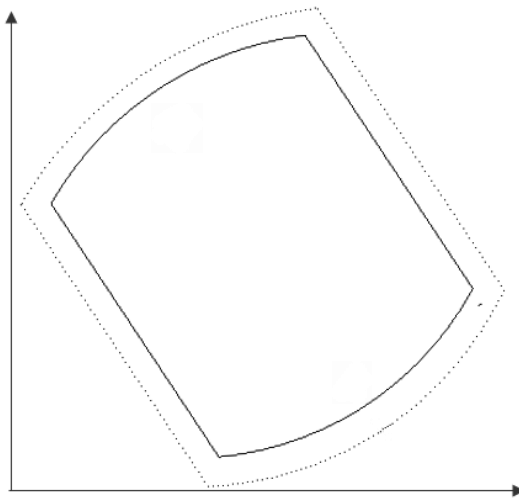
shortage of material occurs during machining. Fig 1.1(c) shows the machining allowance of the part, which is set before machining.



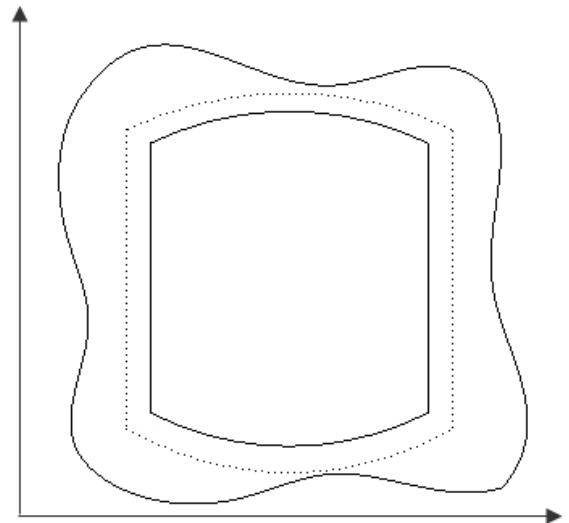
(a) Original location of the raw material



(b) Original location of the reference model
(final part after machining)



(c) The reference model with machining allowance



(d) New location of reference
model after localization

Figure 1.1. Workpiece localization process

In the workpiece localization process, the raw material must have sufficient machining allowance based on the applied machining requirement. In the machining process of complicated parts from casting or forging, the machining allowance has an important effect on the workpiece's machining efficiency, since larger machining allowance requires longer processing time. However, material shortage may happen if the designed machining allowance for the workpiece is too small. Hence, workpiece localization is extremely critical for precise machining when the raw material size and shape are closely specified to the design model to reduce the non-conformance.

The traditional localization methods of checking the machining allowance are by manual measurement. According to the designed model, the nominal dimensions of the raw material are measured and then the location of the machining allowance is assigned and scribed empirically on the raw material. Giving an accurate evaluation is significantly difficult and time-consuming, even though accurate tools and gauges can be used.

In recent years, the competition in the manufacturing industry has become increasingly intense, causing a drop in gross profits of manufacturing companies. In order to survive in the fierce competitive environment, companies are trying to develop and adopt automatic production technology to replace, as much as possible, human intervention. In turn, this leads to improved efficiency and product's accuracy. In order to make the workpiece localization process more efficient, the automatic workpiece localization methods have been developed, which can help avoid the human intervention.

1.2 Automatic Workpiece Localization

The development of technology, such as computer aided design and numerical control, makes the automatic workpiece localization possible to replace the manual measurement. In the automatic localization processes, the reference modeling provides the reference for the localization, while the data of the raw material can be obtained by some measuring instruments.

Before machining, a workpiece localization process should be conducted to ensure that the reference model is totally enclosed in the raw material with enough machining allowance. Even small deviations produced by the raw material manufacturing process can create material shortage and result in rework. When the reference model cannot be entirely enclosed in the raw material, or the machining allowance is insufficient for machining in certain direction, it means the raw material is not acceptable for the designed model. Therefore, the evaluation of the machining allowance is a very important procedure before actual machining.

To process the workpiece localization, data point clouds of the raw material and the reference model are indispensable in transforming the location of the reference model to the raw material. The development of CMM technology and 3D optical metrology makes automatic workpiece localization possible. The point cloud of the raw material can be measured by a CMM machine or a 3D optical scanner. The process can be roughly divided in two main steps. First, a raw material arbitrarily fixed on a machine table is measured by sampling a number of points on the surfaces of the raw material using a touch trigger probe or a laser scanner. Second, the position and orientation, which allows

designed model enclosed in the raw material, is optimized based on the data supplied by the scanned data and the corresponding reference model. Meanwhile, the data point cloud of the reference model can be generated by some CAD softwares, such as Solidworks, Imageware etc.

In recent years, several automatic methods have been developed to evaluate workpiece localization based on the data of point clouds, with the goal of increasing efficiency and accuracy of localization. Through the workpiece localization algorithm, the point cloud of the reference model transforms to the point cloud of the raw material with sufficient machining allowance in each point. The main goal of the workpiece localization process is to determine whether the reference model is totally enclosed in the raw material with the required machining allowance, which leads to no material shortage of the raw material.

1.3 Problem Statement

This paper presents an automatic workpiece localization algorithm for machining of raw material. The new algorithm focuses on the 2D process such as cutting with simpler inputs and shorter processing time compared to other methods which are used for the 3D process.

The simplified inputs contain:

- 1) The measured point cloud dataset of raw material, which is obtained from an optical scanner;

- 2) The point cloud dataset of corresponding reference model, which is generated from the designed model by software.

The new method removes the input of the relationship between dataset of raw material and the reference data, which reduces most of the workload of acquiring data.

The goal of this paper is creating an efficient algorithm with

- 1) Reliable result for workpiece localization;
- 2) Simplified inputs;
- 3) Less human intervention;
- 4) Shorter processing time.

The paper is organized as follows: Section 2 discusses several existing methods of workpiece localization. Section 3 describes the improved workpiece localization algorithm for 2D problem with simplified input and shorter processing time. Section 4 shows the result of the example, which is used to test the algorithm, and concludes the paper.

Chapter 2

Literature Review

2.1 Iterative Closest Point Algorithm

Iterative closest point (ICP) is an algorithm which defines an objective function and constraints to minimize the difference between two point clouds. ICP is often used to reconstruct 2D or 3D surfaces from different sources, in order to evaluate the potential location and material shortage issues.

In the algorithm, one point cloud (usually from the design model) is kept fixed as the reference or target, while the other point cloud, as the source, (usually captured by CMM or 3D optical scanner) is transformed from its original place to best match the reference iteratively. The transformation combines translation and rotation, which minimize the distance from each point of the source database to the reference point cloud step by step.

The ICP algorithms are found in a number of previous researches. Some papers focused on rigid transformation ^{[2][3][4][5][15][16][17][18][19]}, while the others were looking for solution of non-rigid situation ^{[20][21][22][23][24][25]}. For the workpiece localization problem, both the size and the shape of the raw material should not be changed during transformation. Therefore, the rigid ICP-based algorithm should be considered in the workpiece localization.

The inputs of the ICP algorithm include:

- 1) Measurement point cloud;
- 2) Reference point cloud;
- 3) Initial estimation of the transformation to align the source to the reference;
- 4) Criteria for stopping the iterations.

The basic steps of the algorithm are:

- 1) Finding the closest point from the reference point cloud dataset for each point in the measurement point cloud in order to minimize the difference between two point clouds;
- 2) Calculating the transformation matrix which including translation and rotation matrix, using a mean squared error cost function which will best align each measured point to its match found in the previous steps;
- 3) Transforming the measured points using the transformation matrix obtained in step 2;
- 4) Iterating the previous steps until the result fits the criteria.

Chen ^[16] proposed a localization algorithm for constructing a complete surface from different views of an object. When locating multiple overlapping views of an object, an accurate transformation was needed for surface localization in order to combine them. In his research, a localization algorithm was presented for range image localization which works on the images directly. This localization algorithm was based on minimizing the

distance measurement function which was derived from the definition of 3D surface localization. This function does not require a point to point match, which achieves the localization between different views.

Paul ^[15] described an ICP-based algorithm for the accurate and efficient localization of 3D shapes including free-form curves and surfaces. The rate of convergence of this algorithm was quicker compared to the generic nonlinear optimization algorithm. The quaternion-based algorithm was replaced the singular value decomposition (SVD) method, which was usually used in other ICP algorithm, for searching the transformation of the reference model.

Yan ^[17] presented a fast and robust ICP algorithm for workpiece localization problem by exploiting the biometrics application context. This research introduced the “Pre-computed Voxel Closest Neighbors” strategy to improve the speed of the original ICP-based algorithm. In the ICP algorithm, the most time consuming process is linking each point in the measured point cloud in order to find the closest point on the reference point cloud. In their research, the distance from any point in the 3D space to the reference surface was precomputed, and when the distance was needed, it could be directly utilized, which reduced the search time.

Jost ^[18] proposed an accelerated ICP algorithm for fast shape localization. The algorithm accelerated the process by finding multiple solutions in which each solution at the lower level could be successively improved at a higher level of representation. A K-D tree search and a neighbor search method were used for multiple solutions which had been theoretically and experimentally compared in a 3D shape matching test. Using

either the K-D tree search or the neighbor search, multiple solutions speeded up the localization process, which improved the convergence speed and matching quality.

The ICP-based workpiece localization algorithms are widely used with different 2D and 3D geometric data. However, since the basic ICP algorithm uses a mean square function as the objective function, the algorithm cannot push all points in the measurement point cloud out of the reference point cloud, which can cause a shortage of material in certain places. Additionally, the processing time of the ICP algorithm is slower comparing to other algorithms.

2.2 Geometric Algorithms for Workpiece Localization

Chu ^{[26][27][28]} defined a hybrid localization algorithm solved by nonlinear programming for partially finished workpieces. The algorithm first aligned the reference model with the raw material on its finished surfaces. Next, the geometric problem was converted to a nonlinear programming problem with a convex objective function. The transformation of the raw material was aligned with all the unfinished surfaces out of the model to guarantee the allowances for the future machining. For an arbitrarily fixed raw material, the algorithm computed an appropriate solution with high robustness and computational efficiency.

Li et al ^{[1][7][8][9]} developed an alternating variational approach to localize the parts for both general and symmetric workpieces. Firstly, a least square method was used to formulate the localization problem for a general 3D workpiece. The objective function of

the algorithm gave conditions for optimal reference surface points. Then, an iterative approach was developed for solving the workpiece localization problem. While the reference point cloud was fixed, the measurement point cloud transformed to the corresponding reference of the transformation matrix, which in turn provided translation and rotation information. The transformation matrix was obtained from the singular value decomposition method. In each iteration, the algorithm calculated a new transformation matrix and directed the raw material point cloud to move closer to the reference until the localization fits the objective function.

Xu et al ^[29] introduced another geometric algorithm for symmetric workpiece localization. The algorithm used a geometric function for the optimal Euclidean transformation which localized the measured point cloud to the corresponding reference surface point cloud. The reference surface point cloud was given by two nonlinear equations. In the research, formulas for different symmetrical features were described for workpiece localization respectively. Experimental results showed this algorithm was more computationally efficient than the variational algorithm. However, the algorithm could not be applied to discrete symmetric workpiece problems.

Compared to the ICP-based algorithm, the geometric algorithm has shorter processing time and stronger reliability. However, the input of the algorithm includes the relationship linking each point in the raw material point cloud to the reference surface respectively, which involves manual work.

2.3 Feature Based Workpiece Localization Algorithm

A two-step workpiece localization algorithm was introduced by Xudong, Li et al.^{[30][31]} to solve this dilemma. The Principle Component Analysis (PCA) based algorithm was used to roughly localize the measured point cloud closer to the reference point cloud, which reduced the computation time for the future precise localization. Then, a feature-based localization algorithm extracted the proper surface from both point clouds and the measured point cloud to the reference point cloud with sufficient machining allowance. In the paper, an improved cube-dividing-based approach was recommended to extract planes from point cloud. The point cloud was divided into several cubes with corresponding points in them. Next, the algorithm merged these cubes into different feature planes by calculating the relationship of each cube with its neighbor cubes. A constrained localization approach was described to link the feature planes from each point cloud together to achieve the final result with sufficient machining allowance.

The feature based workpiece localization algorithm can potentially solve the material shortage-checking problem. However, the proposed approach is not fully automatic, which required specifying some critical parameters, such as the thresholds for the algorithm. Additionally, it is not useful in the situation where there is no dominating feature plane in the point cloud.

All the algorithms mentioned above required mapping the measured point cloud dataset to the nominal surfaces of the reference model. This input cannot be obtained directly, which means additional human work is required. In this paper, we introduce an

algorithm, which ignores this input in a 2D workpiece localization process. The efficiency of the algorithm is also higher than previous algorithms in a 2D case.

Chapter 3

Development of the Improved Algorithm for Workpiece Localization

3.1 Algorithm Introduction

To evaluate the workpiece localization process successfully, one question must be clarified: Can the designed reference model of a given workpiece be entirely enclosed in the corresponding measured part with enough allowance? If the answer is yes, then the raw material is proved to satisfy the machining process with sufficient stock allowance, and the algorithm will calculate the best location of the part. If the answer is no, it means one or more places of the raw material will be missing material. When machining, without the proper localization, the workpiece will either be scrapped or reworked after being machined correctly. In this case, the algorithm will preferentially push the designed model out of the raw material to satisfy the machining requirements fully and minimize the related rework cost.

To solve this problem, the machining allowance evaluation is accomplished by a two-step localization of the CAD-discretized point cloud and the measured point cloud, as shown in Fig. 3.1. The constraints are needed to push every measurement point outside the reference model in order to ensure sufficient stock allowance when possible.

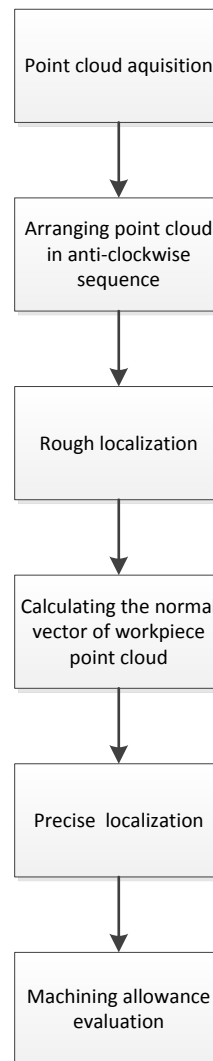


Fig 3.1. Flowchart of machining allowance evaluation.

A point cloud of the raw material could be captured by a laser scanner or Coordinate Measuring Machine (CMM). The point cloud of the raw material is arranged in counter-clockwise sequence, which is used for calculating the normal vector of point cloud later. Then, two point clouds are roughly localized based on Principle Component Analysis (PCA) algorithm. Through calculating normal vectors of lines created by the point with its former point and with latter point, an estimated normal vector of each point in the point cloud is calculated by averaging these two vectors. Next, an iterative least

squares algorithm is introduced for the precise localization. When the minimum distance between the two point clouds is more than the required machining allowance, the iteration stops and a feasible solution is created.

3.2 Preprocessing of Point Cloud Data

In this paper, a filtering process is necessary for the preprocessing of the 3D point cloud which can remove noise points and simplify the point number to increase the computational speed and accuracy ^{[32][33]}. Meanwhile, the reference model is discretized to obtain point cloud by using 3D modeling software (Imageware).

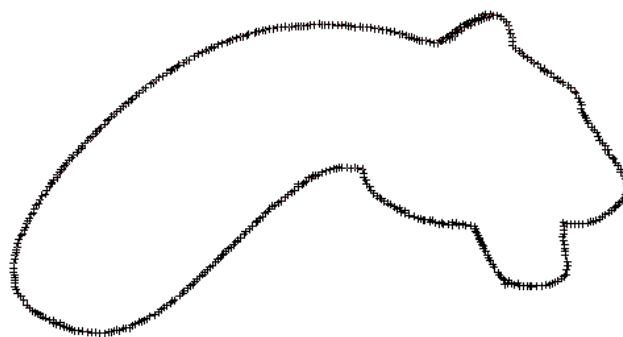
Fig.3.2 shows the part's original scanned data (a), its after-processed point cloud (b), and the discretized reference model(c).

Since the sequence of point stored in the data file is unknown, for the future calculation, the point cloud of the raw material data is arranged in counter-clockwise sequence.

3.3 Rough Localization of Measured Point Cloud

Commonly, the reference point cloud and the scanned point cloud are separately captured, for they are obtained from different points of view, as shown in Fig. 3.2(a). To localize the reference point cloud and the scanned point cloud roughly, a PCA ^{[34][35][36]} based method is used to accomplish the rough localization.

(a) Original scanned data



(b) After-processed data



(c) Discretized reference model

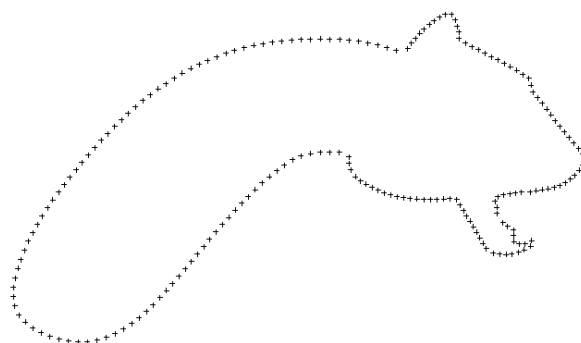


Fig 3.2. Original scanned data (a); After-processed data (b); discretized reference model (c)

Principal component analysis (PCA) is a statistical procedure that uses an orthogonal transformation to convert a set of observations of possibly correlated variables into a set of values of linearly uncorrelated variables called principal components.

The approach of PCA is defined as follow:

Step 1: Input the whole point cloud X ;

Step 2: Calculate the n -dimensional mean vector of each point cloud;

Step 3: Compute the covariance matrix of the standardized dataset.

Standardization of features will have an effect on the outcome of a PCA (assuming that the variables are originally not standardized).

The equation for standardization of a variable is written as

$$Z = \frac{X_i - \bar{X}}{S} \quad (3-1)$$

The original covariance matrix is:

$$\sigma_{xy} = \frac{1}{n-1} \sum_i^n (X_i - \bar{X})(Y_i - \bar{Y}) \quad (3-2)$$

While, $x'_i = \frac{X_i - \bar{X}}{S_x}$ and $y'_i = \frac{Y_i - \bar{Y}}{S_y}$, after standardizing, the covariance

matrix is:

$$\begin{aligned}
s'_{xy} &= \frac{1}{n-1} \sum_i^n (x'_i - 0)(y'_i - 0) \\
s'_{xy} &= \frac{1}{(n-1)s_{xy}} \sum_i^n (x_i - \bar{x})(y_i - \bar{y}) \\
s'_{xy} &= \frac{s_{xy}}{s_x s_y}
\end{aligned} \tag{3-3}$$

Step 4: Compute the eigenvectors and eigenvalues of the covariance matrix

Compute the matrix V of eigenvectors which diagonalizes the covariance

matrix s'_{xy} :

$$V^{-1} S_{xy} V = D \tag{3-4}$$

where D is the diagonal matrix of eigenvalues of σ'_{xy} . This step will typically involve the use of a computer-based algorithm for computing eigenvectors and eigenvalues. These algorithms are readily available as sub-components of most matrix algebra systems, such as R, Matlab;

Step 5: Rearrange the eigenvectors and eigenvalues.

Sort the columns of the eigenvector matrix V and eigenvalue matrix D in order of decreasing eigenvalue. Make sure to maintain the correct pairings between the columns in each matrix.

Step 6: Choose k eigenvectors that correspond to the k largest eigenvalues where k is the number of dimensions of the new feature subspace

In this case, suppose the scanned point cloud is P_s , and the designed reference point cloud is P_c . \bar{P}_s and \bar{P}_c are the center of two point clouds respectively. $\bar{P}_s - \bar{P}_c$ is the vector which translates the scanned point cloud to reference point cloud.

By decomposing its covariance matrix, the point cloud eigenvalues $[\lambda_1, \lambda_2]$ and its corresponding eigenvectors $[\alpha_1, \alpha_2]$ could be calculated. Rotation matrixes of two point clouds are $R_S = [\alpha_{S1}, \alpha_{S2}]$ and $R_C = [\alpha_{C1}, \alpha_{C2}]$. The rotation matrix which transforms P_C to P_S is $R_C R_S^{-1}$.

In the linear algebra a rotation matrix is a matrix that is used to perform a rotation in Euclidean space. Eq. (3-5) shows a counter-clockwise rotation matrix which rotates an angle θ from the original coordinate system.

$$R = \begin{pmatrix} \cos q & -\sin q \\ \sin q & \cos q \end{pmatrix} \quad (3-5)$$

To perform the rotation, the position of each point from point cloud must be represented by a column vector, containing the coordinates of the point. Rotation matrices also provide a means of numerically representing an arbitrary rotation of the axes about the origin, without appealing to angular specification. These coordinate rotations are a natural way to express the orientation of a camera, or the attitude of a spacecraft, relative to a reference axes-set.

3.4 Precise Localization of Measured Point Cloud

As mentioned before, when evaluating precision machining allowance, the scanned point cloud and the reference point cloud are not exactly the same because of the existence of the machining allowance. Hence, a precise localization optimization, which involves a set of scanned points $P_S = \{P_{Si} \mid i = 1, 2, \dots, n\}$ and a set of reference

points $P_C = \{P_{Ci} \mid i = 1, 2, \dots, n\}$ is necessary for the workpiece localization problem.

The least-square principle is introduced to transform the reference point cloud to coincide with the scanned data as close as possible. An objective function F is shown as follows:

$$F = \sum_{i=1}^n \|d_i\|^2 \quad (3-6)$$

where $\|\cdot\|$ is the Euclidean norm distance; d_i is the distance between the scanned point cloud and its corresponding point on the reference point cloud can be calculated with the following function:

$$d_i = |RP_{Si} + T - Q_{Ci}| \quad (3-7)$$

where the point Q_{Ci} is the nearest point on reference point cloud to scanned data point cloud, $T \in \mathbb{R}^3$ is the translation vector that includes t_x and t_y , where t_i is the translation along the i th axis, and $R \in \mathbb{R}^{3 \times 3}$ is the rotation matrix, where q represents the angle of rotation about the axis. The translation vector T and the rotation matrix R describe the rigid transformation of the scanned data related to the reference data respectively.

Let $X = [\theta, t_x, t_y]$ be the transformation variables, then Eq. (3-7) can be written as a function of X with the following expressions:

$$d_i(X) = |R(X)P_{Si} + T(X) - Q_{Ci}| \quad (3-8)$$

Replacing Eq. (3-7) into Eq. (3-5):

$$F(X) = \sum_{i=1}^n \|d_i(X)\|^2 \quad (3-9)$$

The objective function F is calculated as minimization of the summation of squared distances of scanned points in P_S from nearest reference points Q_C with respect to the three rigid transformation parameters included in X . The optimal solution for minimizing the objective function $F(X)$ is the calculated vector X .

For workpiece localization, the vital objective is to push each scanned point out of the reference model in order to make sure that there is sufficient machining allowance for certain workpiece to be machined. Therefore, it is necessary to set effective constraints of oriented Euclidean distances d_i^0 from the scanned points to the reference model.

$$d_i^0 \geq \varepsilon \quad (3-10)$$

where ε is the minimum machining allowance of the given workpiece, and the oriented Euclidean distance d_i^0 can be defined as

$$d_i^0(X) = (R_k(X)P_{sik} + T_k(X) - Q_{cik}) \times n_{ik}^q \quad (3-11)$$

where n_{ik}^q is the unit outward normal vector of the designed reference model at the point Q_{cik} . With this definition, scanned points with negative value between the points and the reference data means insufficient material at these positions and scanned points with positive value represent enough material.

Normally, the workpiece localization problem is focused on minimizing the objective function $F(X)$ with n constraints of oriented Euclidean distance $d_i^0(X) \geq \delta$. The algorithm will converge the scanned data point cloud to a feasible solution if the reference model is entirely within the raw material. Otherwise, it will remind that the raw

material is infeasible in this case. The mathematical model of localization optimization can be described as follows:

$$\begin{aligned} \text{minimize } F(X) &= \sum_{i=1}^n \|d_i(X)\|^2 \\ \text{subject to } d_i^0(X) &\leq \epsilon \end{aligned} \quad (3-12)$$

Applying the transformation, the scanned data point cloud would have the following coordinates:

$$\begin{pmatrix} PX'_{Si} \\ PY'_{Si} \end{pmatrix} = \begin{pmatrix} \cos q & -\sin q \\ \sin q & \cos q \end{pmatrix} \begin{pmatrix} PX_{Si} \\ PY_{Si} \end{pmatrix} + \begin{pmatrix} dx \\ dy \end{pmatrix} \quad (3-13)$$

Substituting Eq. (3-13) into Eq. (3-11):

$$\begin{aligned} d_i^0(q, dx, dy) &= \left(\begin{pmatrix} \cos q & -\sin q \\ \sin q & \cos q \end{pmatrix} \begin{pmatrix} PX_{Si} \\ PY_{Si} \end{pmatrix} + \begin{pmatrix} dx \\ dy \end{pmatrix} \right. \\ &\quad \left. - \begin{pmatrix} QX_{Ci} \\ QY_{Ci} \end{pmatrix} \right) \cdot \begin{pmatrix} nX_i^q \\ nY_i^q \end{pmatrix} \end{aligned} \quad (3-14)$$

Therefore, the Eq.(11) can be expressed as follows:

$$\begin{aligned} \text{minimize } F(q, dx, dy) &= d_i^0(q, dx, dy) \\ \text{subject to } d_i^0(q, dx, dy) &\leq \epsilon \end{aligned} \quad (3-15)$$

If θ is very small (less than 0.03°), in order to simplify the formula and increase the calculating speed, sine and cosine values of θ can be approximated by $\sin q \approx q$ and $\cos q \approx 1$ [37]. Through using these approximations in Eq. (3-14), an equivalent function can be expressed as follows:

$$d_i^0(q, dx, dy) = \begin{pmatrix} 1 & -q \\ q & 1 \end{pmatrix} \begin{pmatrix} PX_{Si} \\ PY_{Si} \end{pmatrix} + \begin{pmatrix} dx \\ dy \end{pmatrix} - \begin{pmatrix} QX_{Ci} \\ QY_{Ci} \end{pmatrix} \cdot \begin{pmatrix} nX_i^q \\ nY_i^q \end{pmatrix} \quad (3-16)$$

A quadratic programming algorithm is used to optimize Eq. (3-11). Quadratic programming (QP) is a special type of mathematical optimization problem. It is the problem of optimizing (minimizing or maximizing) a quadratic function of several variables subject to linear constraints on these variables. The standard function of the algorithm is defined as:

$$\begin{aligned} & \text{minimize } \frac{1}{2} X^T H X + f^T X \\ & \text{subject to } d_i^0(q, dx, dy) \leq e \end{aligned} \quad (3-17)$$

where f is an n-dimensional real vector of first order parameters, H is the Hessian Matrix:

$$H(q, x, y) = \begin{bmatrix} \frac{\partial^2 f}{\partial^2 q^2} & \frac{\partial^2 f}{\partial q \partial x} & \frac{\partial^2 f}{\partial q \partial y} \\ \frac{\partial^2 f}{\partial x \partial q} & \frac{\partial^2 f}{\partial^2 x^2} & \frac{\partial^2 f}{\partial x \partial y} \\ \frac{\partial^2 f}{\partial y \partial q} & \frac{\partial^2 f}{\partial y \partial x} & \frac{\partial^2 f}{\partial^2 y^2} \end{bmatrix} \quad (3-18)$$

The calculation of minimum distances between scanned points and the reference model are an essential and critical step in the phase of optimization. It has an important influence on the computing efficiency of the optimization since large numbers of distance

calculations are required in minimizing objective function. Fig.3.3 shows the flow chart of the workpiece localization algorithm.

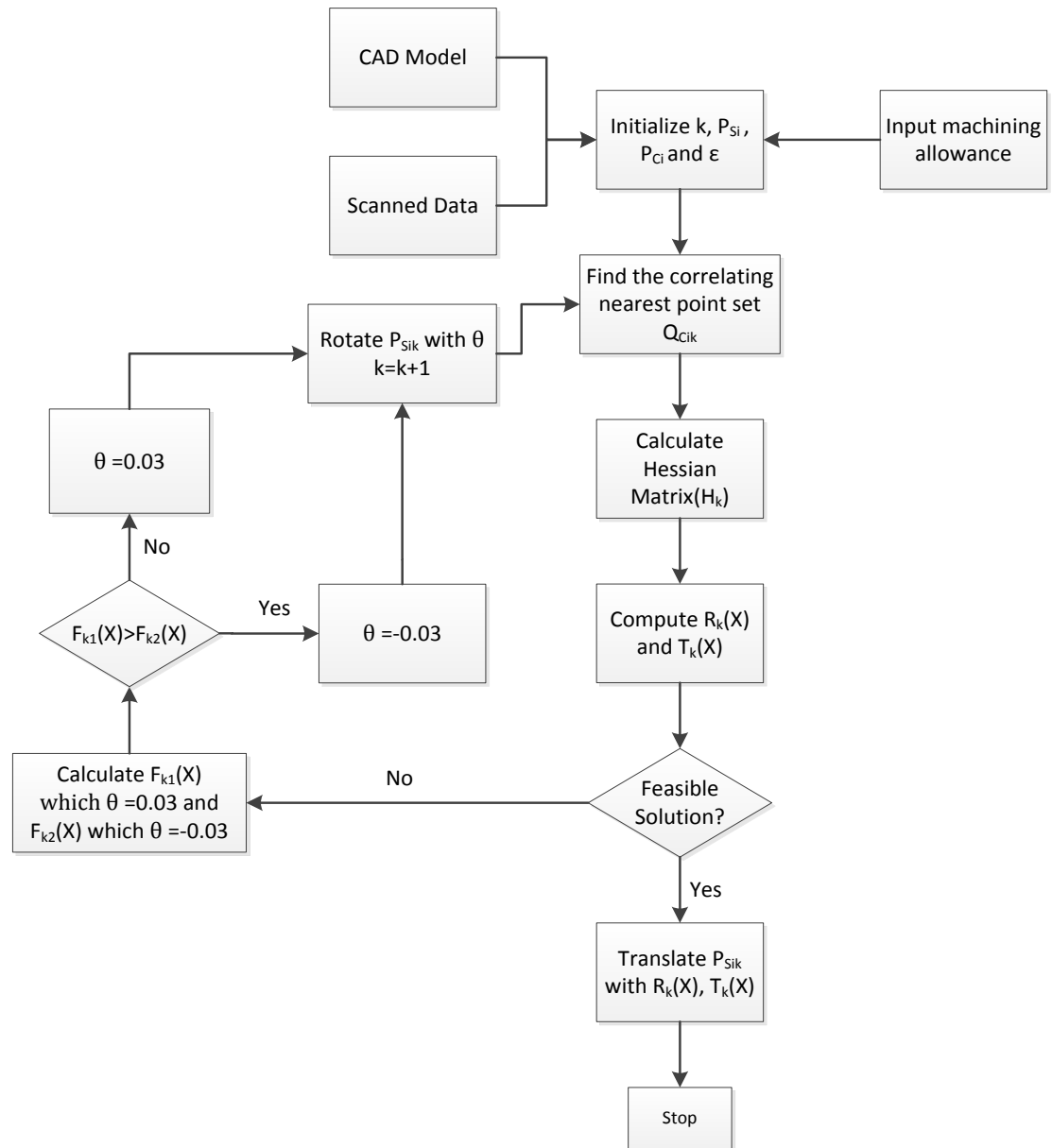


Fig 3.3. Flow chart of the workpiece localization algorithm

Step 0: Initialize the input data P_{Si0} , P_{Ci0} and ε ;

Step 1: Search the nearest point from P_{Ci0} relating to each point in P_{Sik} , and save in data set Q_{Cik} ;

Step 2: Calculate the Hessian Matrix based on Eq. (3-14);

Step 3: Apply QP algorithm to optimize the objective function Eq. (3-11), and get $R_k(X)$, $T_k(X)$;

Step 4: Evaluate the solution. If it is feasible, go to Step 7. Otherwise, go to Step 5;

Step 5: Let absolute value of rotation angle θ_k equal to 0.03° . Calculate $F_k(0.03^\circ)$ and $F_k(-0.03^\circ)$. Then select θ_k with smaller F_k value.

Step 6: Rotate P_{Sik} with angle chosen θ_k to get $P_{Si(k+1)}$, and then go to Step to 1 for next iteration.

Step 7: If the solution is feasible, transform P_{Sik} with $R_k(X)$ and $T_k(X)$. Stop iteration.

Chapter 4

Result and Conclusion

In this chapter, a workpiece localization example of the improved algorithm is shown. The objective of the example is to demonstrate the algorithm. A comparison between the new method and other existing methods is discussed later.

4.1 Example of Workpiece Localization Algorithm

Consider the bottle opener example where the raw material has been cut with plasma arc. After scanning the raw material, the point cloud obtained is shown in figure. The CAD file of the final part is processed through Imageware and point cloud obtained is shown in figure. Since the two point clouds are in different coordinate systems, the superimposition of them in a single co-ordinate frame is shown in Fig. 4.1(a). A machining allowance of 2.5 millimeter is required to be maintained.

A rough localization is used to move the two point clouds closer, in order to reduce the processing time of precise localization. The transformation contains a translation matrix $\overline{P}_S - \overline{P}_C$ and a rotation matrix $R_C R_S^{-1}$. The result of the transformation is shown in Fig. 4.1.

After rough localization, two point clouds are closed. However, there are still some reference points outside the precision casting point cloud, as shown in Fig. 4.1(c), which implies the precise registration is necessary.

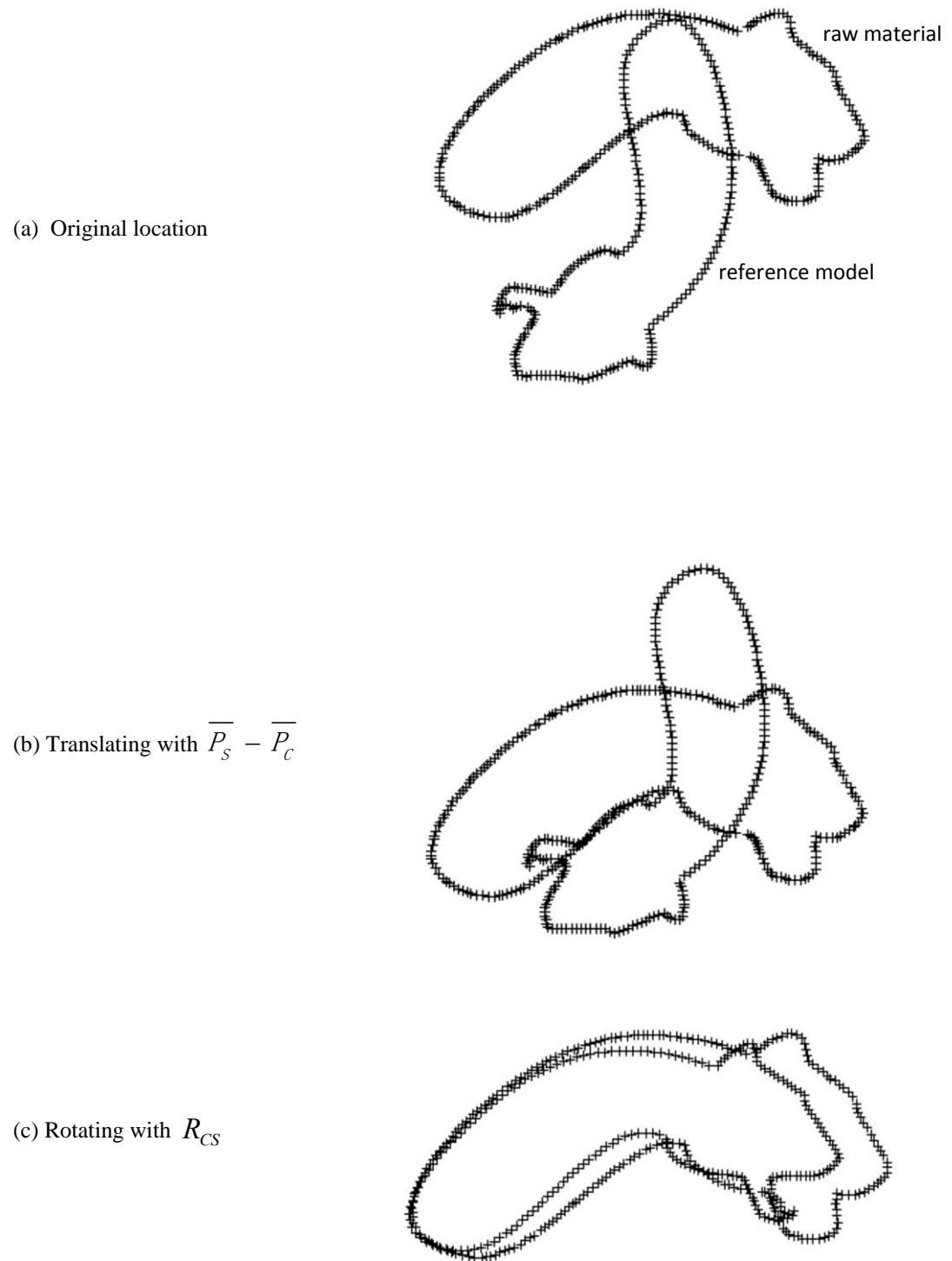


Fig 4.1. Original location (a); center-superposed point clouds (b); rough localization result (c).

Since the structure and the appearance between the reference point cloud and measured point cloud usually vary significantly, a precise localization has to find the relationship between each point in the measured point cloud and the reference point cloud. In the previous research, this relationship should be set before processing the algorithm. In this algorithm, this input can be replaced by estimating the normal vector of reference point cloud after organizing the sequence of the reference point cloud. The normal vector of each point in the reference point cloud could be estimated by calculating the normal vectors with points before and after this point.

The inputs of the bottle opener example only include point clouds of reference model and measured data from equipment, no additional information is required for the algorithm. The result shows in Fig. 4.2.

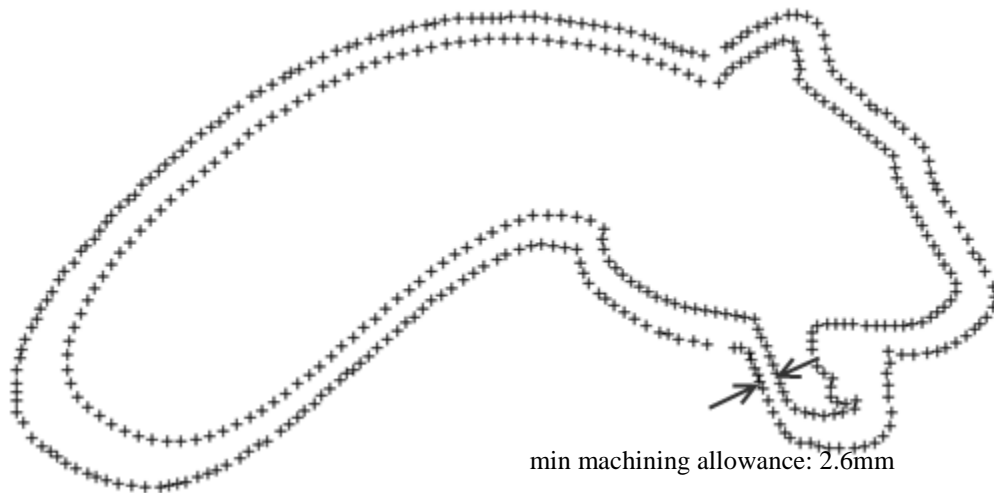


Fig 4.2. Precise localization result

Assuming the machining allowance of 3.0 millimeter is required for this part, which leads to material shortage, the algorithm stops in the last iteration with an infeasible solution, which shows in Fig. 4.3.

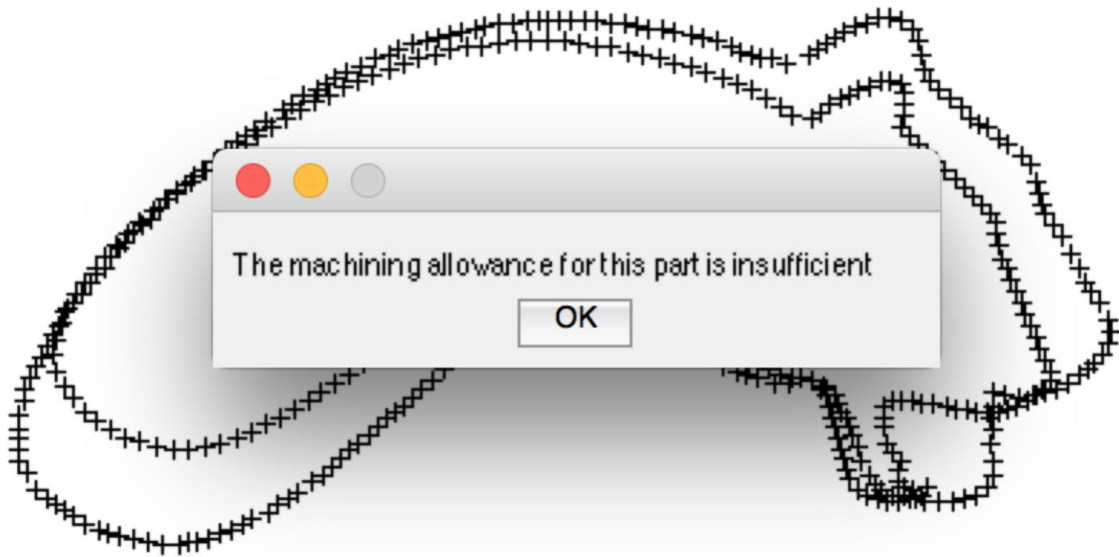


Fig 4.3. Result with insufficient machining allowance

4.2 Comparison of the new algorithm and previous algorithm

For the new workpiece localization algorithm, the inputs are much simpler than the previous algorithm since the relationship between two point clouds and the normal vector of each point in the reference point cloud are not required. Additionally, the new algorithm uses rough localization before precise localization and an approximated Trigonometric function, which increase the calculating speed.

Table 4.1 shows the comparison results between different algorithms. From Table 4.1, the improved least-square method exhibits the significant advantages in computing speed while the accuracy of localization is as same as other algorithms.

Table 4.1 Comparisons between different algorithms.

Method	Iteration Number	Time(s)	Rejected points
Improved LSM	7	3.5	0
Geometric	4	5.8	0
ICP	6	7.3	0

Fig. 4.4 exhibits the comparison of convergence between different methods. Since the improved LSM method uses an approximated Trigonometric function which leads to limited changes in each iteration, the algorithm need more iteration than other methods and the convergence speed is slower.

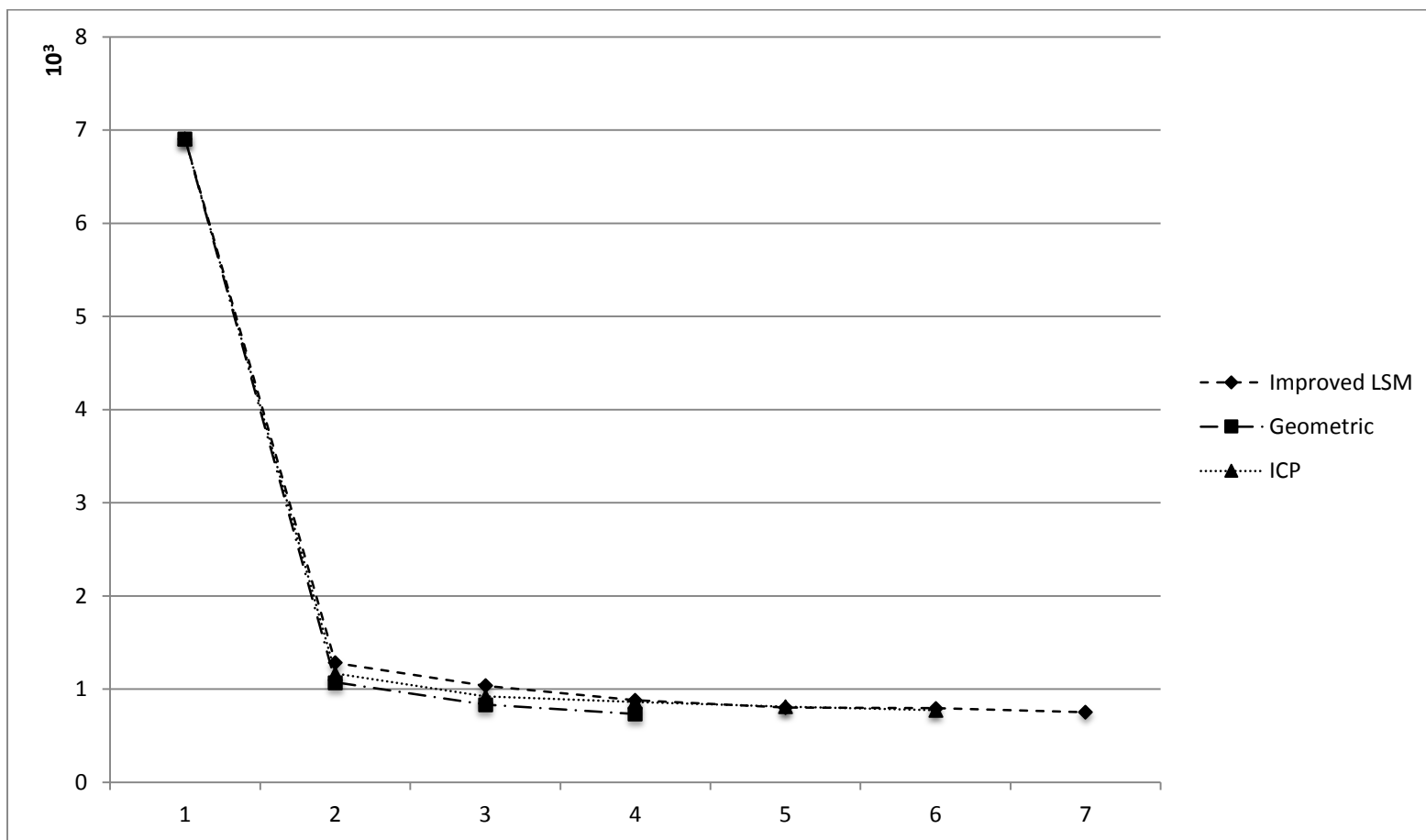


Fig. 4.4. Convergence of different methods

4.3 Conclusion

A new two-step localization algorithm is developed in this paper for localization of workpiece in raw material. It enables avoiding the material shortage of the workpiece. The optimization problem firstly narrows the difference between measured point cloud of the raw material and the point cloud of the reference model by a rough localization in order to reduce the calculation time. Subsequently, a least-square based optimization method is proposed to solve the precise localization. The process converges to a feasible solution under certain constraints, if the machining allowance of the workpiece is sufficient for the designed model. The proposed approach is faster and more automatic than the other algorithms in 2D case. It can improve the efficiency and the possibility of successful workpiece localization, and provides a way to evaluate the machining allowance automatically. The example has shown that the proposed algorithm can be effectively used in workpiece localization in raw material checking. The processing time of the improved algorithm is much faster than the previous algorithms in 2D workpiece localization process. The simplified inputs reduce most human intervention during workpiece localization. The future efforts will be placed on extending the algorithm from 2D to 3D cases by arranging the points in a well-organized sequence. Additionally, the tolerance of the parts should be considered in the future work to avoid rejecting feasible workpiece.

References

- [1] Li, Xiaomin, Maurice Yeung, and Zexiang Li. "An algebraic algorithm for workpiece localization." *Robotics and Automation*, 1996. Proceedings., 1996 IEEE International Conference on. Vol. 1. IEEE, 1996.
- [2] Zhang, Zhengyou. "Iterative point matching for registration of free-form curves and surfaces." *International journal of computer vision* 13.2 (1994): 119-152.
- [3] Rusinkiewicz, Szymon, and Marc Levoy. "Efficient variants of the ICP algorithm." *3-D Digital Imaging and Modeling*, 2001. Proceedings. Third International Conference on. IEEE, 2001.
- [4] Xu, Jinting, et al. "Accurate and efficient algorithm for the closest point on a parametric curve." *Computer Science and Software Engineering, 2008 International Conference on*. Vol. 2. IEEE, 2008.
- [5] Xu, Jinting, Jianhuang Wu, and Wenbin Hou. "Parts Localization Oriented Practical Method for Point Projection on Model Surfaces Based on Subdivision." *Computer-Aided Design and Applications* 12.1 (2015): 67-75.
- [6] Jinting, Xu. "Algorithm for free-form surface matching based on curvatures." *JOURNAL OF COMPUTER AIDED DESIGN AND COMPUTER GRAPHICS* 19.2 (2007): 193.
- [7] Li, Zexiang, Jianbo Gou, and Yunxian Chu. "Geometric algorithms for workpiece localization." *Robotics and Automation, IEEE Transactions on* 14.6 (1998): 864-878.

- [8] Gou, Jianbo, Yunxian Chu, and Zexiang Li. "On the symmetric location problem." *Robotics and Automation, IEEE Transactions on* 14.4 (1998): 533-540.
- [9] Chu, Yunxian. Workpiece localization: Theory, algorithms and implementation. Hong Kong University of Science and Technology (People's Republic of China), 1999.
- [10] Chatelain, Jean-Fran çois. "A level-based optimization algorithm for complex part localization." *Precision engineering* 29.2 (2005): 197-207.
- [11] Chatelain, J. F., and C. Fortin. "A balancing technique for optimal blank part machining." *Precision engineering* 25.1 (2001): 13-23.
- [12] Yuwen, Sun, et al. "Machining localization and quality evaluation of parts with sculptured surfaces using SQP method." *The International Journal of Advanced Manufacturing Technology* 42.11-12 (2009): 1131-1139.
- [13] Sun, Yu-wen, et al. "A unified localization approach for machining allowance optimization of complex curved surfaces." *Precision engineering* 33.4 (2009): 516-523.
- [14] Rong, Yu, Jinting Xu, and Yuwen Sun. "A surface reconstruction strategy based on deformable template for repairing damaged turbine blades." *Proceedings of the Institution of Mechanical Engineers, Part G: Journal of Aerospace Engineering* (2013): 0954410013517091.
- [15] Besl, Paul J., and Neil D. McKay. "Method for registration of 3-D shapes." *Robotics-DL tentative*. International Society for Optics and Photonics, 1992.
- [16] Chen, Yung, and Gérard Medioni. "Object modeling by registration of multiple range images." *Robotics and Automation, 1991. Proceedings., 1991 IEEE International Conference on*. IEEE, 1991.

- [17] Yan, Ping, and Kevin W. Bowyer. "A fast algorithm for ICP-based 3D shape biometrics." *Computer Vision and Image Understanding* 107.3 (2007): 195-202.
- [18] Jost, Timothy, and Heinz Hugli. "A multi-resolution scheme ICP algorithm for fast shape registration." *3D Data Processing Visualization and Transmission, 2002. Proceedings. First International Symposium on*. IEEE, 2002.
- [19] Chetverikov, Dmitry, et al. "The trimmed iterative closest point algorithm." *Pattern Recognition, 2002. Proceedings. 16th International Conference on*. Vol. 3. IEEE, 2002.
- [20] Feldmar, Jacques, et al. "Extension of the ICP algorithm to non-rigid intensity-based registration of 3D volumes." *Mathematical Methods in Biomedical Image Analysis, 1996., Proceedings of the Workshop on*. IEEE, 1996.
- [21] Haehnel, Dirk, Sebastian Thrun, and Wolfram Burgard. "An extension of the ICP algorithm for modeling nonrigid objects with mobile robots." *IJCAI*. Vol. 3. 2003.
- [22] Chui, Haili, and Anand Rangarajan. "A new point matching algorithm for non-rigid registration." *Computer Vision and Image Understanding* 89.2 (2003): 114-141.
- [23] Amberg, Brian, Sami Romdhani, and Thomas Vetter. "Optimal step nonrigid icp algorithms for surface registration." *Computer Vision and Pattern Recognition, 2007. CVPR'07. IEEE Conference on*. IEEE, 2007.
- [24] Dragomir Anguelov, Praveen Srinivasan, et al. "The correlated correspondence algorithm for unsupervised registration of nonrigid surfaces." *Advances in Neural Information Processing Systems 17: Proceedings of the 2004 Conference*. Vol. 17. MIT Press, 2005.

- [25] Myronenko, Andriy, Xubo Song, and Miguel A. Carreira-Perpinán. "Non-rigid point set registration: Coherent point drift." *Advances in Neural Information Processing Systems*. 2006.
- [26] Chu, Y. X., J. B. Gou, and Z. X. Li. "On the hybrid workpiece localization/envelopment problems." *Robotics and Automation, 1998. Proceedings. 1998 IEEE International Conference on*. Vol. 4. IEEE, 1998.
- [27] Chu, Yunxian. *Workpiece localization: Theory, algorithms and implementation*. Hong Kong University of Science and Technology (People's Republic of China), 1999.
- [28] Chu, Y. X., J. B. Gou, and Z. X. Li. "Workpiece localization algorithms: Performance evaluation and reliability analysis." *Journal of manufacturing systems* 18.2 (1999): 113-126.
- [29] Yi, Xu, Limin Ma, and Zexiang Li. "A geometric algorithm for symmetric workpiece localization." *Intelligent Control and Automation, 2008. WCICA 2008. 7th World Congress on*. IEEE, 2008.
- [30] Li, Xudong, et al. "Automatic evaluation of machining allowance of precision castings based on plane features from 3D point cloud." *Computers in Industry* 64.9 (2013): 1129-1137.
- [31] Li, Xudong, et al. "A registration method based on profile matching for vegetation canopy measurement." *SPIE/COS Photonics Asia*. International Society for Optics and Photonics, 2014.
- [32] Bae, K-H., D. Belton, and D. D. Lichti. "Pre-processing procedures for raw point clouds from terrestrial laser scanners." *Journal of Spatial Science* 52.2 (2007): 65-74.

- [33] Schall, Oliver, Alexander Belyaev, and Hans-Peter Seidel. "Robust filtering of noisy scattered point data." *Point-Based Graphics, 2005. Eurographics/IEEE VGTC Symposium Proceedings*. IEEE, 2005.
- [34] Jolliffe, Ian. Principal component analysis. John Wiley & Sons, Ltd, 2002.
- [35] Wold, Svante, Kim Esbensen, and Paul Geladi. "Principal component analysis." *Chemometrics and intelligent laboratory systems* 2.1 (1987): 37-52.
- [36] Moore, Bruce C. "Principal component analysis in linear systems: Controllability, observability, and model reduction." *Automatic Control, IEEE Transactions on* 26.1 (1981): 17-32.
- [37] Cheraghi, S. H., E. A. Lehtihet, and P. J. Egbelu. "Vision-assisted lead-to-pad alignment technique for placement of surface mount components." *IIE transactions* 27.4 (1995): 473-482.

Appendix A

Dataset of Original Point Clouds

Original CAD Data	X	Y		X	Y
1	151.0353	8.4415	101	204.7407	48.9715
2	150.2534	9.4298	102	202.6953	49.3692
3	150.8125	10.7832	103	200.6469	49.752
4	151.0988	12.0376	104	198.5948	50.1141
5	150.684	14.3957	105	196.5385	50.4511
6	149.9955	15.4869	106	194.4777	50.7595
7	142.1793	13.5012	107	192.4124	51.0359
8	143.2578	54.1772	108	190.3424	51.2755
9	141.9174	54.5767	109	188.2678	51.4718
10	140.5541	54.8888	110	186.1891	51.6164
11	139.1728	55.1077	111	184.1071	51.6971
12	137.7798	55.2334	112	182.0235	51.6958
13	136.3817	55.2684	113	179.9428	51.5846
14	134.9843	55.2091	114	177.8774	51.3158
15	133.5941	55.0567	115	175.8606	50.8
16	132.2172	54.8115	116	173.9775	49.9156
17	131.1108	53.9279	117	172.2238	48.7911
18	131.3593	52.5522	118	170.5562	47.5423
19	131.8036	51.2269	119	168.9635	46.1989
20	132.4205	49.9727	120	156.6118	23.3043
21	133.2119	48.8207	121	157.8035	24.121
22	145.4716	55.5387	122	158.9574	24.9904
23	146.6328	57.2692	123	160.0888	25.889
24	147.8678	58.9473	124	161.2043	26.8073
25	149.177	60.5681	125	162.3011	27.7484
26	150.558	62.1284	126	163.3621	28.7287
27	152.0059	63.6268	127	164.3609	29.7721
28	153.5135	65.0648	128	165.2887	30.8795
29	155.0722	66.4476	129	166.1498	32.0395
30	156.6727	67.7822	130	166.9394	33.2493
31	158.3062	69.0761	131	167.6478	34.5082
32	159.9712	70.3289	132	168.2733	35.8104

33	161.669	71.537	133	168.8447	37.1377
34	163.4007	72.6959	134	169.3251	38.4995
35	165.1673	73.801	135	169.5821	39.9186
36	166.9695	74.8467	136	169.4134	41.6358
37	168.8081	75.827	137	168.8603	42.9664
38	170.6834	76.7351	138	168.0152	44.1356
39	172.5945	77.5653	139	151.218	4.51
40	174.5379	78.3167	140	152.532	4.9323
41	176.5094	78.99	141	153.7791	5.523
42	178.5055	79.5863	142	154.9287	6.2861
43	180.5231	80.1069	143	155.9552	7.2081
44	182.5587	80.5528	144	156.8426	8.2653
45	184.6092	80.9256	145	157.4277	9.9455
46	186.6712	81.2263	146	157.2267	11.3122
47	188.7421	81.4564	147	157.0206	12.6778
48	190.8196	81.6173	148	156.819	14.0441
49	192.9013	81.7103	149	156.6167	15.4102
50	194.9847	81.7375	150	156.4107	16.7758
51	197.0682	81.7029	151	156.2076	18.1419
52	199.1499	81.6106	152	156.0129	19.5092
53	201.2282	81.4651	153	155.7962	20.8731
54	203.3024	81.2705	154	155.6434	22.2439
55	205.3721	81.031	155	151.7655	7.3436
56	207.4372	80.7508	156	151.1761	6.2316
57	209.4972	80.434	157	150.2455	5.3944
58	211.5518	80.0847	158	148.6781	5.1077
59	213.601	79.7069	159	149.6279	4.2705
60	215.6456	79.3045	160	143.7578	14.6332
61	217.6857	78.8804	161	144.8438	15.3103
62	219.7202	78.4297	162	145.9416	15.9681
63	221.7465	77.9438	163	147.0648	16.5811
64	223.7618	77.4143	164	148.2481	17.0626
65	225.7628	76.8328	165	149.4516	16.6603
66	227.7455	76.1916	166	128.642	11.3107
67	229.7051	75.4836	167	129.8484	10.76
68	231.6368	74.7026	168	131.119	10.3689
69	233.5352	73.8435	169	132.4261	10.1299
70	235.3944	72.9031	170	133.7536	10.063
71	237.2089	71.8791	171	135.0799	10.1518
72	238.9736	70.7712	172	136.3833	10.4106
73	240.674	69.567	173	137.6298	10.8691

74	242.2617	68.2193	174	138.8003	11.4991
75	243.6491	66.6679	175	139.926	12.2072
76	244.6791	64.8631	176	141.0794	12.8687
77	245.1676	62.8446	177	132.739	47.2144
78	245.1313	60.7655	178	132.1331	45.7664
79	244.6862	58.7329	179	131.5216	44.3207
80	243.9338	56.791	180	130.9066	42.8764
81	242.9439	54.9587	181	130.2909	41.4325
82	241.7598	53.2451	182	129.678	39.9874
83	240.4075	51.6608	183	129.0716	38.5396
84	238.9016	50.2218	184	128.4755	37.0874
85	237.2486	48.9549	185	127.8932	35.6297
86	235.4529	47.9009	186	127.3308	34.1643
87	233.5372	47.0846	187	126.9719	32.6412
88	231.5373	46.5036	188	127.4996	31.2161
89	229.4865	46.138	189	128.0174	29.7614
90	227.4112	45.958	190	128.1335	28.1966
91	225.3279	45.9292	191	128.1611	26.6271
92	223.2462	46.0174	192	128.1804	25.0575
93	221.1696	46.1895	193	128.1987	23.4879
94	219.0986	46.4196	194	128.2134	21.9182
95	217.0337	46.699	195	128.222	20.3486
96	214.975	47.0208	196	128.2215	18.7789
97	212.922	47.3773	197	128.2086	17.2092
98	210.8735	47.7596	198	128.1792	15.6398
99	208.8283	48.1586	199	128.1443	14.0705
100	206.7845	48.5654	200	128.2021	12.5023

Original Data of Workpiece	X	Y		X	Y
1	72.4654	56.2088	114	-14.311	21.9501
2	73.7031	55.4543	115	-15.759	21.4669
3	74.8374	54.1012	116	-18.0396	20.6611
4	75.1913	52.4154	117	-19.2036	20.358
5	74.9706	50.4494	118	-20.9366	19.847
6	74.8709	48.6349	119	-22.4612	19.3105
7	74.9088	46.9821	120	-24.6251	19.0438
8	75.777	45.658	121	-26.1108	18.8368
9	76.6382	44.1114	122	-27.5341	18.6856

10	77.73	42.6055	123	-29.0593	18.635
11	78.5826	40.8644	124	-30.7208	18.4178
12	79.2872	39.9444	125	-32.1561	18.511
13	80.3669	38.9998	126	-33.2698	18.8168
14	81.2205	37.4403	127	-34.5527	18.8642
15	82.2169	36.208	128	-36.6035	19.5122
16	83.3634	34.4365	129	-38.3831	20.242
17	84.1363	32.8714	130	-40.049	21.1139
18	84.3509	30.7329	131	-41.6872	22.0673
19	83.9614	29.1755	132	-42.754	22.8996
20	84.047	27.6287	133	-43.7984	23.6338
21	84.2281	26.3707	134	-45.2174	24.8347
22	84.6162	24.5673	135	-46.3752	26.1345
23	85.1772	22.8763	136	-47.428	27.3648
24	85.73	20.4027	137	-48.1022	28.3603
25	86.2227	18.3939	138	-48.9875	29.3626
26	86.5131	16.456	139	-49.8923	31.0396
27	86.9114	15.1242	140	-50.4544	33.2958
28	87.2948	13.3643	141	-50.8942	35.0478
29	87.6964	11.0584	142	-50.5586	36.6334
30	87.5118	9.4123	143	-50.1823	37.764
31	86.8828	8.1834	144	-49.8614	39.0191
32	85.66	7.0953	145	-49.1694	40.8418
33	84.4146	6.3992	146	-48.1906	42.38
34	83.3747	5.874	147	-47.5254	43.4748
35	82.1071	5.4239	148	-46.6658	44.725
36	80.4245	4.9174	149	-45.3998	46.1228
37	78.7467	4.5416	150	-44.3584	47.0682
38	77.3662	4.5091	151	-43.2869	48.1821
39	75.8749	4.6019	152	-42.1916	49.1963
40	74.0554	5.0249	153	-40.9662	50.0954
41	72.3387	5.672	154	-39.6112	51.4567
42	70.8316	6.5755	155	-38.4522	52.3344
43	70.3313	4.9451	156	-36.9452	53.0505
44	69.5997	3.5442	157	-35.3426	54.2652
45	69.3743	1.9479	158	-34.3863	54.8605
46	68.8387	0.3218	159	-33.0963	55.4885
47	68.52	-1.8897	160	-31.9656	56.4016
48	67.8088	-3.5607	161	-30.725	57.3315
49	66.5222	-4.8959	162	-29.7586	57.8617
50	64.8858	-5.2847	163	-28.2184	58.7279

51	63.5063	-5.3379	164	-26.7492	59.3128
52	61.9775	-5.1752	165	-25.536	59.7455
53	59.9912	-4.6541	166	-24.2609	60.6712
54	58.4607	-4.1777	167	-22.8578	61.2942
55	57.2723	-3.5799	168	-21.4074	61.8769
56	56.2313	-2.6639	169	-20.1112	62.5626
57	54.8726	-2.2123	170	-18.6908	63.1351
58	53.7276	-1.1361	171	-17.3549	63.7951
59	53.2244	-0.1115	172	-15.8122	64.4372
60	52.8269	1.1033	173	-13.9699	65.1325
61	52.3637	3.2414	174	-12.2848	65.7676
62	52.1853	4.9106	175	-10.962	66.1191
63	52.0072	6.6979	176	-9.5865	66.8
64	51.9205	7.8169	177	-7.7579	67.3766
65	51.8437	8.9238	178	-5.5112	68.0646
66	51.7162	10.0279	179	-4.1581	68.4067
67	51.6085	11.1256	180	-2.2736	68.9132
68	51.5998	12.2374	181	-0.3331	69.3449
69	50.7795	13.1671	182	0.8468	69.6398
70	49.8744	13.5834	183	2.0016	69.8473
71	46.2548	15.2219	184	3.9394	70.2249
72	44.4156	16.1279	185	5.8881	70.4674
73	42.6291	17.1341	186	7.8889	70.7428
74	41.2282	18.1873	187	9.7185	70.7436
75	40.3171	18.8803	188	11.0419	70.9513
76	38.7253	20.1703	189	13.0642	71.0171
77	37.2661	21.6226	190	14.7963	70.9679
78	36.2238	23.0616	191	16.3506	71.0905
79	35.1824	24.3606	192	17.9102	70.8545
80	34.2045	25.7076	193	19.3535	70.875
81	33.5204	26.5963	194	21.2328	70.6579
82	32.641	28.4628	195	22.4825	70.5256
83	32.27	30.1887	196	24.1496	70.374
84	32.2851	31.6198	197	25.9882	70.0231
85	32.4827	33.6072	198	27.816	69.5903
86	30.8995	34.4095	199	29.2131	69.1165
87	29.2844	35.0477	200	30.5007	68.7206
88	27.7026	35.7748	201	31.7788	68.3624
89	26.3712	35.9298	202	33.1554	68.1245
90	24.5558	36.0016	203	35.0508	67.5032
91	22.6018	35.8828	204	36.3616	67.0135

92	21.0556	35.5807	205	37.9988	66.3416
93	18.9978	35.1667	206	39.7333	65.6257
94	17.3914	34.7307	207	41.0559	64.8165
95	15.7298	34.2275	208	42.5694	64.1037
96	13.6896	33.5818	209	44.1126	63.5481
97	11.9837	32.9994	210	45.7031	62.7601
98	10.4122	32.7334	211	47.3954	61.8946
99	8.9903	32.0607	212	48.9985	60.936
100	7.4303	31.2754	213	50.6071	59.9467
101	6.0936	30.8288	214	51.9694	58.9497
102	4.5154	30.1429	215	53.0224	57.8404
103	2.6414	29.4559	216	54.0541	57.0937
104	1.0169	28.6349	217	55.1575	56.3693
105	-0.469	27.9461	218	56.4826	55.6783
106	-1.88	27.3041	219	57.9101	54.5828
107	-3.2049	26.7683	220	61.2567	54.8183
108	-4.3515	26.3942	221	62.5168	55.0823
109	-5.4889	25.7703	222	63.7904	55.5568
110	-7.1208	24.9703	223	64.9944	55.9208
111	-8.6186	24.4558	224	66.441	56.2067
112	-9.965	23.7547	225	67.9303	56.4443
113	-11.4687	23.2166	226	69.4447	56.5674
114	-12.8407	22.5932	227	71.1826	56.5903

Appendix B

Code of the Algorithm

```

function pointset = scan_anticlockwise(pointset)
for i = 1:size(pointset,1)
    for j = i+1:size(pointset,1)
        if (atan2(pointset(i,2)-0.5,pointset(i,1)-0.5) >
atan2(pointset(j,2)-0.5,pointset(j,1)-0.5));
            temp = pointset(i,:);
            pointset(i,:) = pointset(j,:);
            pointset(j,:) = temp;
        end
    end
end
Error=2.5;
contour1=xlsread('LIONdata','CAD');
CAD=contour1';
CAD(1,:)=CAD(1,:);
CAD(2,:)=CAD(2,:);
CAD=flipud(CAD);
contour2=xlsread('LIONdata','Blank');
contour3=contour2;
contour2=contour2';
R=[cos(0.3),-sin(0.3);
    sin(0.3),cos(0.3)];
contour2=R*contour2;
Scan=contour2;
CA=cov(CAD');
CB=cov(Scan');
Scanx=mean(Scan(1,:));
Scany=mean(Scan(2,:));
Scan(1,:)=Scan(1,:)-Scanx;
Scan(2,:)=Scan(2,:)-Scany;
contour2=Scan;
[A1,D1]=eig(CA);
[B1,D2]=eig(CB);
B2=B1^(-1);
R=A1*B2;
CAD2=CAD'*R;
CAD2=CAD2';
CADx=mean(CAD2(1,:));
CADy=mean(CAD2(2,:));
CCAD(1,:)=CAD2(1,:)-CADx;
CCAD(2,:)=CAD2(2,:)-CADy;
QNumber=size(CCAD,2);
SNumber=size(Scan,2);
CR1=contour2(1,:);

```

```

CR2=contour2(2,:);
CR3=CR1(end: -1:1);
CR4=CR2(end: -1:1);
Anticlockwise_Scan(1,:)=CR3;
Anticlockwise_Scan(2,:)=CR4;
for NNumber=1:SNumber
    if NNumber==SNumber
        n_vector(1,NNumber)=(Anticlockwise_Scan(2,1)-
Anticlockwise_Scan(2,NNumber))/norm(Anticlockwise_Scan(:,NNumber)-
Anticlockwise_Scan(:,1));
        n_vector(2,NNumber)=-(Anticlockwise_Scan(1,1)-
Anticlockwise_Scan(1,NNumber))/norm(Anticlockwise_Scan(:,NNumber)-
Anticlockwise_Scan(:,1));
    else
        n_vector(1,NNumber)=(Anticlockwise_Scan(2,NNumber+1)-
Anticlockwise_Scan(2,NNumber))/norm(Anticlockwise_Scan(:,NNumber)-
Anticlockwise_Scan(:,NNumber+1));
        n_vector(2,NNumber)=-(Anticlockwise_Scan(1,NNumber+1)-
Anticlockwise_Scan(1,NNumber))/norm(Anticlockwise_Scan(:,NNumber)-
Anticlockwise_Scan(:,NNumber+1));
    end
end
for VNumber=1:SNumber
    if VNumber==1
        n_vector2(1,VNumber)=(n_vector(1,1)+n_vector(1,SNumber));
        n_vector2(2,VNumber)=(n_vector(2,1)+n_vector(2,SNumber));
        Nnorm=norm(n_vector2(:,VNumber));
        n_vector2(1,VNumber)=n_vector2(1,VNumber)/Nnorm;
        n_vector2(2,VNumber)=n_vector2(2,VNumber)/Nnorm;
    else
        n_vector2(1,VNumber)=(n_vector(1,VNumber)+n_vector(1,VNumber-
1));
        n_vector2(2,VNumber)=(n_vector(2,VNumber)+n_vector(2,VNumber-
1));
        Nnorm=norm(n_vector2(:,VNumber));
        n_vector2(1,VNumber)=n_vector2(1,VNumber)/Nnorm;
        n_vector2(2,VNumber)=n_vector2(2,VNumber)/Nnorm;
    end
end
tempN=n_vector;
n_vector=n_vector2;
for i=1:QNumber
    PCAD=CCAD(:,i);
    Cor=[PCAD,Anticlockwise_Scan]';
    d=pdist(Cor);
    D=squareform(d);
    LineQ=D(1,2:size(D,1));
    Dmin=min(LineQ);
    [m,lm]=find(LineQ==Dmin);
    Q(:,i)=Anticlockwise_Scan(:,lm);
    n(:,i)=n_vector(:,lm);
end
for k=1:10
    H=[sum((CCAD(2,:).^2+CCAD(1,:).^2),sum((-
CCAD(2,:)),sum(CCAD(1,:)));

```

```

        sum((-CCAD(2,:)),size(CCAD,2),0;
        sum(CCAD(1,:), 0, size(CCAD,2)];
f=[2*sum((-Q(1,:)).*CCAD(2,:))+((-Q(2,:)).*CCAD(1,:)));
  2*sum((CCAD(1,:)-Q(1,:)));
  2*sum((CCAD(2,:)-Q(2,:)))]];
A=[n(1,:).*CCAD(2,:)-n(2,:).*CCAD(1,:;-n(1,:;-n(2,:)]];
A=A';
b=[Q(1,:).*n(1,:)-n(1,:).*CCAD(1,:)+Q(2,:).*n(2,:)-
n(2,:).*CCAD(2,:)-Error];
b=b';
[Solution,fval,exitflag]=quadprog(H,f,A,b);
Output(1,k)=fval;
if exitflag==1
    if Solution(1,1)<=0.1 && Solution(1,1)>=-0.1
        R2=[cos(Solution(1,1)),sin(Solution(1,1));-
sin(Solution(1,1)),cos(Solution(1,1))];
        CCAD=R2*CCAD;
        Temp1=CCAD;
        CCAD(1,:)=CCAD(1,:)-Solution(2,1);
        CCAD(2,:)=CCAD(2,:)-Solution(3,1);
    else
        R2=[1-0.01^2,0.01;-0.01,1-0.01^2];
        CCAD=R2*CCAD;
        Temp1=CCAD;
        CCAD(1,:)=CCAD(1,:)-Solution(2,1);
        CCAD(2,:)=CCAD(2,:)-Solution(3,1);
    end
    for i=1:QNumber
        PCAD=CCAD(:,i);
        Cor=[PCAD,Anticlockwise_Scan]';
        d=pdist(Cor);
        D=squareform(d);
        LineQ=D(1,2:size(D,1));
        Dmin=min(LineQ);
        [m,lm]=find(LineQ==Dmin);
        Temp2=Q;
        Q(:,i)=Anticlockwise_Scan(:,lm);
        n(:,i)=n_vector(:,lm);
    end
    for j=1:size(CCAD,2)
        if sum((Q(:,j)-CCAD(:,j)).*n(:,j))<Error
            flag=1;
            CCAD=Temp1;
            Q=Temp2;
            break
        else
            flag=2;
        end
    end
    if flag==2
        break
    end
else
    R3=[cos(pi/180),sin(pi/180);-sin(pi/180),cos(pi/180)];
    CCAD=R3*CCAD;

```

```

CCAD(1,:)=CCAD(1,:)-Solution(2,1);
CCAD(2,:)=CCAD(2,:)-Solution(3,1);
for i=1:QNumber
    PCAD=CCAD(:,i);
    Cor=[PCAD,Anticlockwise_Scan]';
    d=pdist(Cor);
    D=squareform(d);
    LineQ=D(1,2:size(D,1));
    Dmin=min(LineQ);
    [m,lm]=find(LineQ==Dmin);
    Q(:,i)=Anticlockwise_Scan(:,lm);
    n(:,i)=n_vector(:,lm);
end
end
end
if exitflag==2
    msgbox('There is enough machining allowance for the part')
else
    msgbox('No enough machining allowance for the part')
end

plot(Anticlockwise_Scan(1,:),Anticlockwise_Scan(2,:),'+k')
axis equal
hold on
plot(CCAD(1,:),CCAD(2,:),'+k')
hold off
axis([-80 80 -50 50]);

```